Carotid Artery Segmentation on Ultrasound Image using Deep Learning based on Non-Local Means-based Speckle Filtering

by Aji Sapta Pramulen

Submission date: 26-Apr-2022 12:06PM (UTC+0800)
Submission ID: 1820548412
File name: ep_Learning_based_on_Non-Local_Means-based_Speckle_Filtering.pdf (629.12K)
Word count: 3254
Character count: 16932

Carotid Artery Segmentation on Ultrasound Image using Deep Learning based on Non-Local Means-based Speckle Filtering

Aji Sapta Pramulen
Department of Electrical Engineering
Institut Teknologi Sepuluh Nopember
Surabaya, Indonesia
aji.19071@mhs.its.ac.id

Eko Mulyanto Yuniarno
Department of Electrical Engineering
Department of Computer Engineering
UCE AIHeS
Institut Teknologi Sepuluh Nopember
Surabaya, Indonesia
ekomulyanto@ee.its.ac.id

J. Nugroho
Department of Cardiology
Airlangga University
Surabaya, Indonesia
j.nugroho.eko@fk.unair.ac.id

I Made Gede Sunarya
Department of Informatic Engineering of Education
Universitas Pendidikan Ganesha
Singaraja, Indonesia
sunarya@undiksha.ac.id

I Ketut Eddy Purnama *)
Department of Electrical Engineering
Department of Computer Engineering
UCE AIHeS
Institut Teknologi Sepuluh Nopember
Surabaya, Indonesia
ketut@ee.its.ac.id

***Abstract*— Cardiovascular disease (CVD) causes significant deaths worldwide, of which 17.3 million deaths per year are due to CVD. The use of Ultrasound is necessary to see the abnormalities. The study will segment Carotid Artery segmentation on the Ultrasound image by using the U-Net- based architecture of non-local means-based speckle filtering (NLMBSF). The images will use NLMBSF to reduce speckles, and the data set will be divided into two parts, namely the dataset, which using NLMBSF and not NLMBSF. After that, doing training to create a U-net model, the training data model results will be searched with the best Accuracy. The obtained result of the study is an accuracy value of 97.74%, dice value is 87.22%, and a loss of 0.0107 on data that does not use NLMBSF. Still, it got different data results using NLMBSF, namely 97.6% accuracy, dice value is 84.06% and 0.0138 value loss.**

***Keywords*— Ultrasound, U-Net, Segmentation, Carotid Artery**

I. Introduction

Cardiovascular disease causes significant deaths worldwide, of which 17.3 million deaths per year are due to CVD and is expected to increase by 23.6 million in 2030. In 2008, cardiovascular deaths represented 30% of all deaths globally, of which 80% occurred in developing countries. Developing countries like Indonesia obtained data on the prevalence of coronary heart disease in 2013 by 0.5% or 883,447 people and symptoms by

1.5% or around 2,650,340 people, where the data based on doctor's diagnosis [1]. Carotid Intima-Media Thickness (CIMT) is a measurement of carotid artery intima-media thickness by B-mode ultrasonography, where the examination technique is non-invasive sensitive. CIMT is useful for the identification and quantification of subclinical CVD and for evaluating CVD risk. CIMT, as an early sign of atherosclerosis, is associated with the risk factors for cardiovascular events, CVD, and the occurrence of arteriosclerosis in peripheral and coronary arteries [2].

The use of Ultrasonography due to this image has gained much popularity due to its low cost and non-invasive nature, allowing rapid assessment of vessel geometry, degree of stenosis, and morphological plaque [3]. The Framingham risk score can be used to identify high-risk individuals without symptoms. The multifactorial risk index is based on traditional risk factors such as hypercholesterolemia, diabetes mellitus, hypertension, age, and smoking. Calcium assessment, Ankle Brachial Index (ABI), C-reactive Protein (CRP)) and carotid ultrasound (USG) to measure CIMT thickness ([4], [8]).

In a study conducted (Yang, Ji et al. [4]) using Dual-Path U-Net, the Accuracy was 4% -5% higher than that of Seg-Net and U-Net using an intravascular dataset from Ultrasound. Intravascular modalities can only be obtained because they require Ultrasound, which must be inserted into the body and inserted into the vessels. On the other hand, in this study, Dual-Path U-net uses small datasets because of the availability of intravascular datasets and dataset limitations but produces good Accuracy. Research by (Azzopardi, et.all, [5]) used Geometrically Constrained, which was added to the Deep Convolutional Neural Network, namely the U-Net. The weakness of this study is that it is very dependent on an expert to do the labelling used for dataset training. Research conducted by (Zhou Y, Zang H, [6]) proposed a Non-local means-based speckle filtering algorithm to reduce the presence of speckles in ultrasound modalities. The results of this study produce good CNR and SNR values compared to the original data and make faster computational time from this algorithm. NLMBSF method is very efficient at smoothing homogeneous areas while preserving edges ([9],[10]). Research conducted by (Li, Xiaomeng [11]) produced segmentation results from Liver and Tumor in CT Volume

*)Corresponding Author

using Hybrid Densely Connected U-NET with products shown better Accuracy of the architecture. This research has weaknesses in architecture that have to use a high CPU type because the computing used is very time-consuming. The study conducted by (Sancho-Gomez et al. [12]) used Machine Learning and Statistical Pattern Recognition in the segmentation of Carotid, where this study featured in terms of high-speed computing, which is 1.4 second with the lowest average error. In this study, segmentation was longitudinal without the use of transverse.

To reduce the spackle and improve the previous research, the research to be carried out is to segment the Carotid Artery on Ultrasound images using U-Net architecture based on Non-local means-based speckle filtering (NLMBSF). In this study, the images will use NLMBSF to reduce speckles. After speckles reduce the image, the data set will be divided into two parts: the dataset, which uses NLMBSF, and not NLMBSF. Each dataset will be divided into training and testing data. Manual masking will be done to perform labels used for training. After that, it will continue into the segmentation process.

II. MATERIALS AND METHOD

A. *Preparation Data*

Artery B-Mode ultrasound data were acquired using the Ultrasound Telemed SmartUs EXT-1M modality and Echowave II software. Ultrasound data was taken on a lab-scale and handled directly by researchers. Data is taken from several different people. The data taken is in the form of a video that will be converted to frame form and removed information from the device. After manual segmentation is used to create a label on the dataset, where the label will be used for training. Data Training and Testing. The total data used is 150, where 90 data are used for training, 10 data for validation of training, and 50 data for testing. Furthermore, Figure 1(a) and Figure 1(c) show that the image used for this study while Figure 1(b) and Figure 1(d) shows the masked image

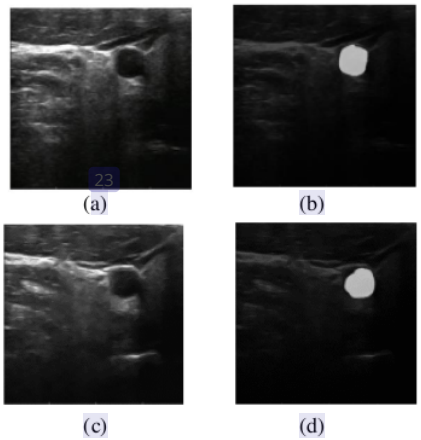

Fig. 1. Visualization of Data Training : (a) Original Image, (b) Mask of Original Image, (c) Image after NLMBSF, and (d) Mask of Image after NLMBSF

B. *Preprocessing*

Frame in the form of an image will be preprocessed by performing NLMBSF, which reduces speckle and noise in the existing structures [6]. NLMBSF assumes the intensity of each pixel is related to the pixel intensity of the entire image. As a practical and computational reason, the number of pixels in the weighted average is limited. As illustrated in (1). The restored intensity $NL(u)(x_i)$ of the pixel x_i, is weighted average at pixel intensity $u(x_i)$ in the "search volume." V_i.

$$NL(u)(x_i) = \sum_{x_j \in V_i} w(x_i, x_j) u(x_j) \quad (1)$$

Where $w(x_i, x_j)$ is a weight applied to the intensity value $u(x_j)$ for restoration for each pixel x_i in V_i, the Gaussian-weighted Euclidean distance $\|.\|^2_{2,a}$ is calculated between the two image patches $u(N_j)$ and $u(N_j)$. This distance is the traditional $L2 - norm$ wrapped around a standard deviation Gaussian kernel. The Gaussian kernel is standard deviations peruse to establish spatial weights, which aim to patch elements. Compared to pixels located at the edges, it turns out that the middle pixel in the patch contributes more to the distance. The weight $w(x_i, x_j)$ is then calculated using equation (2) below.

$$w(x_i, x_j) = \frac{1}{Z_i} \exp - \frac{\|u(N_i) - u(N_j)\|^2_{2,a}}{h^2} \quad (2)$$

$\sum_{x_j \in V_i} w(x_i, x_j) = 1$ confirmed as a normalization constant symbolized by Z_i , where h acts as a smoothing parameter. The algorithm used was to follow the equation described (Zhou et al., 2019) [6]. The results from NLMBSF are converted into an image size to 128 x 128 pixels and make a mask from the existing image into a range [0, 1].

C. *Model*

In recent years, a deep convolutional network has outstripped state of the art on many visual recognition tasks, e.g. [13]. Convolution Network has been around for a long time[14]. Still, the success factor of the limited Convoluted Network is based on the size of the existing training dataset as well as the size of the network that is considered. Since then, a more comprehensive and deeper network has been trained. The typical use of convolutional networks is on classification tasks, where the output to the image is a single class label [13]. Research conducted by Ciresan et al. [15] has completed training on the network, which aims to set a sliding window to predict class labels on each pixel with inputs that are local areas (patches) around pixels.

The model used is a convolutional auto-encoder, but with a twist, it jumps over the connection from the encoder layer to the decoder layer that is at the same "level." See Figure 2. Deep neural networks are implemented with a Keras functional API, making it very easy to use to realize any desired architecture. The output of the system is 64 x 80, which represents the Mask must be training. The Sigmoid activation function ensures that the pixel mask is within the range [0, 1].

D. *Segmentation Evaluation Matrics*

To quantitatively measure the segmentation accuracy, two regional-based measures. The Dice coefficient (DICE) [16], also called the overlap index is,

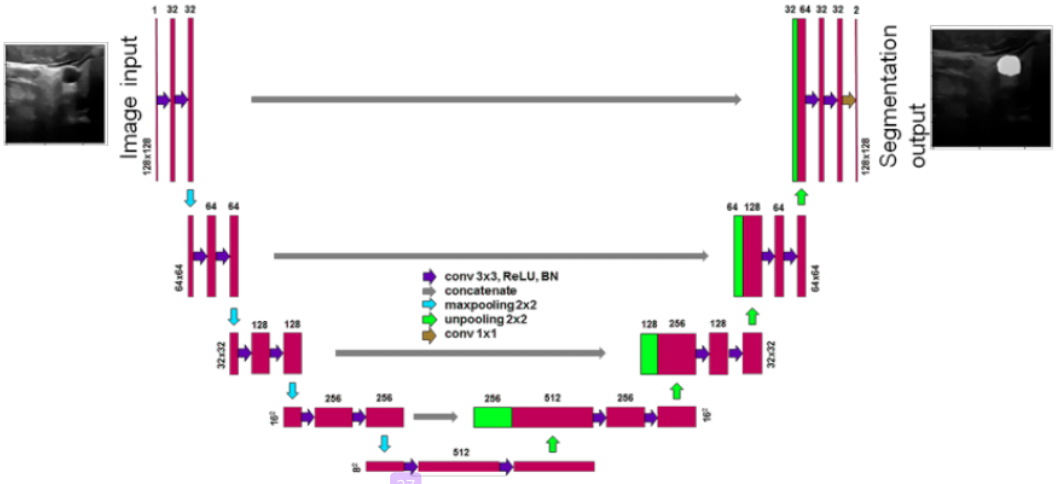

Fig 2. U-Net Architecture [19]

the most used in validating medical segmentations. As a direct comparison between ground truth segmentation and automatic, it is common to use DICE to measure reproductivity. Use of DICE as a reproductive measure [17] as a form of validation of manual annotation statistics with segmenters repeatedly annotating with the same ultrasound image, then the pair-wise overlap of segmentation performed repeated calculations using DICE, which is defined by

$$DICE = \frac{2(S_a|S_b)}{|S_a|+|S_b|} \quad (3)$$

Here S_a is the segmentation result of the algorithm used and S_b is the ground truth.

III. EXPERIMENT SETUP AND RESULT

This research was conducted on a computer-based on Anaconda with the processor specification of Intel Core i7-9750H and NVIDIA GeForce GTX 1650. The training and testing data that has been made will be divided into 2, namely the training and testing data with NLMBSF and the training and testing data without NLMBSF. Figure 2(a) shows the results of the data non- NLMBSF and Figure 2(b) shows the results of the data using NLMBSF. The results of using the NLMBSF Method show more smooth looks as previously done in previous studies for other biomedical imaging ([9],[10]). This method will further clarify the absence of a carotid artery in Ultrasound than other organs.

After training of the data that has been carried out by NLMBSF, it shows in Figure 5. The loss value decreases at epoch 7 with the best deal at epoch 50. In the training process, the model will be stored in the best loss value. Using a model that has produced the smallest loss value, the best segmentation will be created. However, for training data non- NLMBSF is shown in Figure 4. The loss value decreases at epoch 10 with the best loss value on the 4th epoch. After testing, the result showed 97.74% for Accuracy and loss of 0.01056 for data that did not use NLMBSF. However, the different results were obtained for data using NLMBSF, namely 97.6% accuracy and 0.0111 loss value.

The results obtained are better if the image does not use NLMBSF, but the difference between the values is only 0.1. Besides, the Dice Coefficient's value from this study is shown in Table I, and the results of the Dice for training data shown in Figure 6 for non-NLMBSF data and Figure 7 for NLMBSF data. These results indicate that U-Net delivers a good performance in segmenting carotid artery ultrasound.

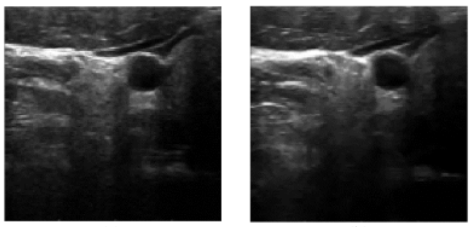

(a) (b)

Fig 3. Dataset : (a) the data non- NLMBSF and (b) data using NLMBSF

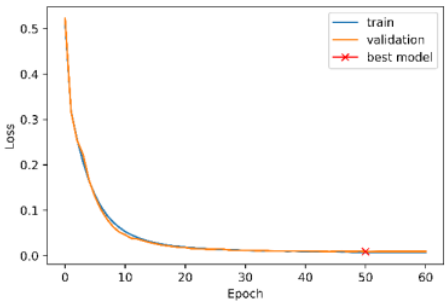

Fig 4. Loss Graph on Training Data non-NLMBSF

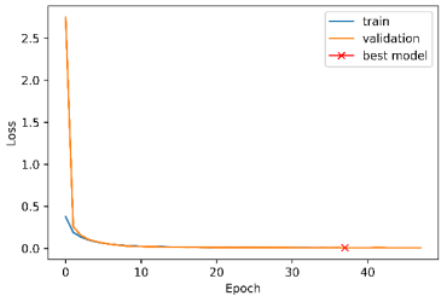

Fig 5. Loss Graph on Training Data NLMBSF

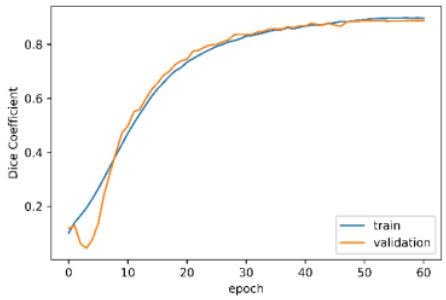

Fig 6. DICE Graph on Training Data non-NLMBSF

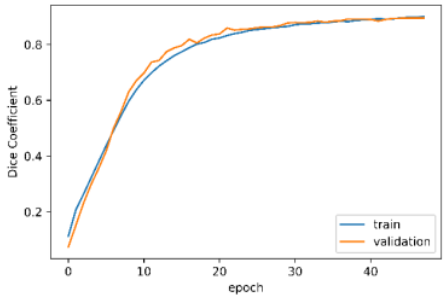

Fig 7. DICE Graph on Training Data NLMBSF

The result of Dice that was approaching 100 shows that the results of segmentation are getting better. DICE more often measure system performance through cross-validation.

$$Accuracy = \frac{TP+TN}{TP+FP+FN+TN} \quad (4)$$

Part of an image pixel that is appropriately classified or expressed as Accuracy [18], where TP, FP, FN, and TN stands for true positive, false positive, false negative, and true negative. It is the most basic performance metric but cannot distort image segmentation performance in case of class imbalance. In such a case, higher Accuracy for the dominating class will overshadow the lower Accuracy associated with the other level, thus providing biased results.

The results of the segmentation are compared with ground truth, which shows in Figure 8 is the result of segmentation on data non-NLMBSF, and Figure 9 is the

Table I. Evaluation Matrics of Data

Data	NLMBSF			Non-NLMBSF		
	Accuracy	Loss	Dice	Accuracy	Loss	Dice
Training	97.60%	0.0108	85.50%	97.74%	0.0076	88.79%
Validation	97.61%	0.0125	84.82%	97.70%	0.0088	88.32%
Testing	97.60%	0.0138	84.06%	97.74%	0.0107	87.22%

result of data using NLMBSF. These two results show good performance in filtering, and it can be seen in the figure that the prediction results and ground truth are similar. This figure will show that the qualitative test by looking at the segmentation result is good.

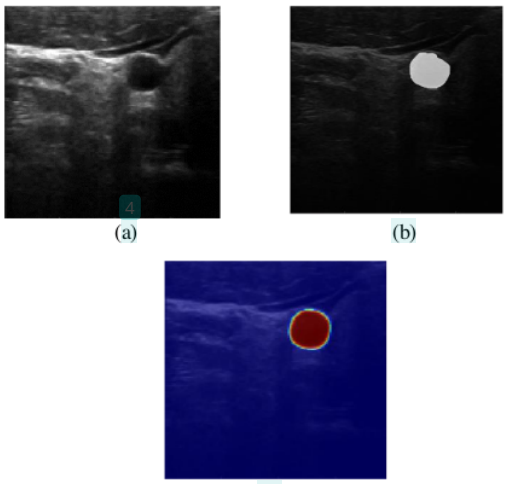

(a) (b) (c)

Fig. 8. The results of the segmentation on Testing Data non-NLMBSF : (a) Image non-NLMBSF, (b) True Mask Image, and (c) Predict Mask

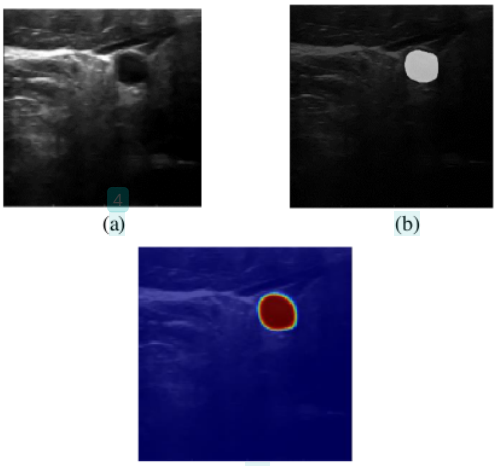

(a) (b) (c)

Fig. 9. The results of the segmentation on Testing Data NLMBSF : (a) Image with NLMBSF, (b) True Mask Image, and (c) Predict Mask

This study, testing of the performance segmentation model, is used for crop images. This Crop image aims to see how good a model is at imaging Carotid Artery and removing the other part. It was intended to demonstrate

how well these results are so that the research can reconstruct carotid artery imagery in the future. Figure 10(a) shows an Image from Ultrasound that Carotid Artery still has another organ, then Figure 10(b) shows the cropping results using a mask created for labelling.

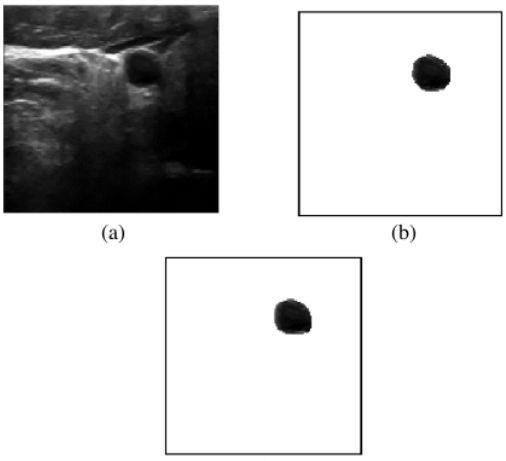

(a) (b)

(c)

Fig. 10. The results of the Cropped non-NLMBSF : (a) Image non-NLMBSF, (b) Cropped Image from True Mask, and (c) Cropped Image from Predict Mask

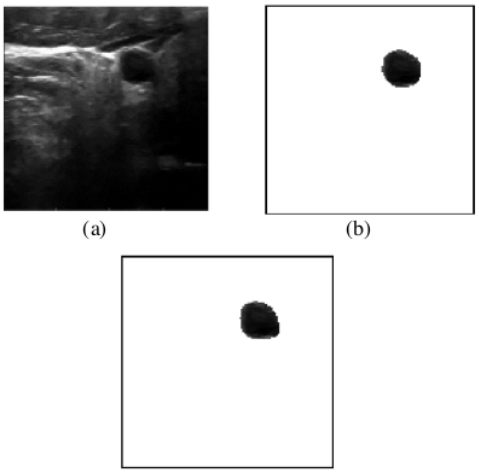

(a) (b)

(c)

Fig. 11. The results of the Cropped NLMBSF : (a) Image NLMBSF, (b) Cropped Image from True Mask, and (c) Cropped Image from Predict Mask

In contrast, Figure 10(c) shows the crop results using predictions from U-Net segmentation. Experiments were also conducted with crop Image with NLMBSF as seen Figure 11(a) showing the Image of Ultrasound that Carotid Artery still has other organs, then Figure 11(b) shows the cropping results using a mask created for labelling. In contrast, Figure 11(c) shows the crop results using predictions from U-Net segmentation. Figure 10 and Figure 11 show that segmentation using U-Net looks pretty good when used for cropping leaving the desired organ, so it not only produces good Accuracy and dice values, but good results are obtained after implementation for a crop.

IV. CONCLUSION

In this study, the accuracy value is 97.74%, dice value is 87.22% and a loss of 0.0107 on data that did not use NLMBSF, but obtained different results for data using NLMBSF, namely 97.6% accuracy, dice value is 84.06%, and 0.0111 loss value. On the other hand, good results were obtained from the results of the ultrasound segmentation, which had been compared with ground truth. This result was proven by trying segmentation and crop Carotid Ultrasound. Future research will be conducted to increase the amount of data so that the variation of the data will increase in terms of disease, sex, and age. This problem causes the conditions of the Carotid to be different so that the variation will increase.

REFERENCES

[1] Badan Penelitian dan Pengembangan Kesehatan. 2013. Riset Kesehatan Dasar 2013. Kementrian Kesehatan Republik Indonesia, Jakarta.

[2] del Sol AI, Moons KG, Hollander M, Hofman A, Koudstaal PJ, Grobbee DE, Breteler MM, Witteman JC, Bots ML. Is carotid intima-media thickness useful in cardiovascular disease risk assessment? The Rotterdam Study. Stroke. 2001 Jul;32(7):1532-8.

[3] Z. Akkus et al., "Fully automated carotid plaque segmentation in combined contrast-enhanced and B-mode ultrasound," Ultrasound Med. Biol., vol. 41, no. 2, pp. 517–531, 2015

[4] Yang J, Faraji M, Basu A. Robust segmentation of arterial walls in intravascular ultrasound images using Dual-Path U-Net. Ultrasonis. 2019 Jul 1;96:24-33.

[5] Azzopardi C, Camilleri K, Hicks YA. Bimodal Automated Carotid Ultrasound Segmentation Using Geometrically Constrained Deep Neural Networks. IEEE Journal of Biomedical and Health Informatics. 2020 Jan 9.

[6] Zhou Y, Zang H, Xu S, He H, Lu J, Fang H. An iterative speckle filtering algorithm for ultrasound images based on bayesian non-local means filter model. Biomedical Signal Processing and Control. 2019 Feb 1;48:104-17.

[7] M. Young, The Technical Writer's Handbook. Mill Valley, CA: University Science, 1989.

[8] Naik, V., Gama, R.S., and Bansod, P.P., 2013. Carotid artery segmentation in ultrasound images and measurement of intima-media thickness. BioMed research international, 2013.

[9] Coupé, P., Hellier, P., Kervrann, C., and Barillot, C., 2009. Non-local means-based speckle filtering for ultrasound images. IEEE transactions on image processing, 18(10), pp.2221-2229.

[10] Coupé, P., Hellier, P., Kervrann, C., and Barillot, C., 2008, May. Bayesian non-local means-based speckle filtering. In 2008 5th IEEE International Symposium on Biomedical Imaging: From Nano to Macro (pp. 1291-1294). IEEE.

[11] Li, X., Chen, H., Qi, X., Dou, Q., Fu, C.W. and Heng, P.A., 2018. H-DenseUNet: hybrid densely connected UNet for liver and tumor segmentation from CT volumes. IEEE transactions on medical imaging, 37(12), pp.2663-2674.

[12] Menchón-Lara, R.M., and Sancho-Gómez, J.L., 2015. Fully automatic segmentation of ultrasound common carotid artery images based on machine learning. Neurocomputing, 151, pp.161-167.

[13] Bruzzone, M.G., D'Incerti, L., Farina, L.L., Cuccarini, V., and Finocchiaro, G., 2012. CT and MRI of brain tumors. The quarterly journal of nuclear Medicine and molecular imaging: official publication of the Italian Association of Nuclear Medicine (AIMN)[and] the International Association of Radiopharmacology (IAR),[and] Section of the Society of..., 56(2), pp.112-137.

[14] Deng, L., and Yu, D., 2014. Deep learning: methods and applications. Foundations and trends in signal processing, 7(3–4), pp.197-387.

[15] Adams, R., and Bischof, L., 1994. Seeded region growing. IEEE Transactions on pattern analysis and machine intelligence, 16(6), pp.641-647.

[16] Dice, L.R., 1945. Measures of the amount of ecologic association between species. Ecology, 26(3), pp.297-302.

[17] Li, X., Hong, Y., Kong, D., and Zhang, X., 2019. Automatic segmentation of levator hiatus from ultrasound images using U-net with dense connections. Physics in Medicine & Biology, 64(7), p.075015.

[18] Haque, I.R.I., and Neubert, J., 2020. Deep learning approaches to biomedical image segmentation. Informatics in Medicine Unlocked, 18, p.100297.

[19] Ronneberger, O., Fischer, P., and Brox, T., 2015, October. U-net: Convolutional networks for biomedical image segmentation. In International Conference on Medical image computing and computer-assisted intervention (pp. 234-241). Springer, Cham.

Carotid Artery Segmentation on Ultrasound Image using Deep Learning based on Non-Local Means-based Speckle Filtering

ORIGINALITY REPORT

19%	11%	15%	0%
SIMILARITY INDEX	INTERNET SOURCES	PUBLICATIONS	STUDENT PAPERS

PRIMARY SOURCES

1	Intisar Rizwan I Haque, Jeremiah Neubert. "Deep learning approaches to biomedical image segmentation", Informatics in Medicine Unlocked, 2020 Publication	1%
2	"The 10th International Conference on Computer Engineering and Networks", Springer Science and Business Media LLC, 2021 Publication	1%
3	Xiaoqing Jiang, Yueli Li, Chongyi Fan, Xiaotao Huang. "An Interpolated Iterative Adaptive Approach for Scanning Radar Imaging", 2019 IEEE International Conference on Signal Processing, Communications and Computing (ICSPCC), 2019 Publication	1%
4	core.ac.uk Internet Source	1%

5	I Made Gede Sunarya, Muhammad Rusydi Al Affan, Arief Kurniawan, Eko Mulyanto Yuniarno. "Digital Map Based on Unmanned Aerial Vehicle", 2020 International Conference on Computer Engineering, Network, and Intelligent Multimedia (CENIM), 2020 Publication	1 %
6	www-o.ntust.edu.tw Internet Source	1 %
7	Fernanda Palhano Xavier de Fontes, Guillermo Andrade Barroso, Pierrick Coupé, Pierre Hellier. "Real time ultrasound image denoising", Journal of Real-Time Image Processing, 2010 Publication	1 %
8	Carl Azzopardi, Yulia A. Hicks, Kenneth P. Camilleri. "Automatic Carotid ultrasound segmentation using deep Convolutional Neural Networks and phase congruency maps", 2017 IEEE 14th International Symposium on Biomedical Imaging (ISBI 2017), 2017 Publication	1 %
9	repository.uin-malang.ac.id Internet Source	1 %
10	www.tqwba.com Internet Source	1 %

11	donsak.sru.ac.th Internet Source	1 %
12	Greeshma Sai Sree Duggireddy, Komali Dammalapati, Y Sravya, S.K. Afroz, K Triinayanaa. "Sequential Convolutional Neural Network based Face Mask Detection", 2021 3rd International Conference on Advances in Computing, Communication Control and Networking (ICAC3N), 2021 Publication	1 %
13	Arik Kurniawati, Yoyon Kusnendar Suprapto, Eko Mulyanto Yuniarno. "Multilayer Perceptron for Symbolic Indonesian Music Generation", 2020 International Seminar on Intelligent Technology and Its Applications (ISITIA), 2020 Publication	1 %
14	www.pharmacytimes.com Internet Source	1 %
15	Asymptomatic Atherosclerosis, 2011. Publication	<1 %
16	Joko Priambodo, Eko Mulyanto Yuniarno, I. Ketut Eddy Purnama. "Magnetic Tracker Calibration Using Polynomial Fitting", 2018 International Seminar on Intelligent Technology and Its Applications (ISITIA), 2018 Publication	<1 %

17	St. Clair, L.. "Biological Surrogates for Enhancing Cardiovascular Risk Prediction in Type 2 Diabetes Mellitus", The American Journal of Cardiology, 20070219 Publication	<1 %
18	Candra Adi Wirawan, Sandi Alfa Wiga Arsa. "Development of Guide Basic Life Support (BLS) Application Based on Android to Increase Accuracy Compression Ritme And Ventilation to Handling of Out Hospital Cardiac Arrest", Babali Nursing Research, 2020 Publication	<1 %
19	S. Nemirovsky-Rotman, Z. Friedman, D. Fischer, A. Chernihovsky, K. Sharbel, M. Porat. "Simultaneous compression and speckle reduction of clinical breast and fetal ultrasound images using rate-fidelity optimized coding", Ultrasonics, 2021 Publication	<1 %
20	Zishang Kong, Min He, Qianjiang Luo, Xiansong Huang et al. "Multi-Task Classification and Segmentation for Explicable Capsule Endoscopy Diagnostics", Frontiers in Molecular Biosciences, 2021 Publication	<1 %
21	"Deep Learning in Medical Image Analysis and Multimodal Learning for Clinical Decision	<1 %

Support", Springer Science and Business Media LLC, 2018
Publication

22	Zhan, Yi, Xuming Zhang, Mingyue Ding, and Sébastien Ourselin. "", Medical Imaging 2012 Image Processing, 2012. Publication	<1 %
23	"Medical Image Computing and Computer Assisted Intervention – MICCAI 2018", Springer Science and Business Media LLC, 2018 Publication	<1 %
24	hdl.handle.net Internet Source	<1 %
25	research.chalmers.se Internet Source	<1 %
26	www.patientcareonline.com Internet Source	<1 %
27	Joanna Czajkowska, Pawel Badura, Szymon Korzekwa, Anna Płatkowska-Szczerek. "Automated segmentation of epidermis in high-frequency ultrasound of pathological skin using a cascade of DeepLab v3+ networks and fuzzy connectedness", Computerized Medical Imaging and Graphics, 2022 Publication	<1 %

28	Luis Pizarro, Pavel Mrázek, Stephan Didas, Sven Grewenig, Joachim Weickert. "Generalised Nonlocal Image Smoothing", International Journal of Computer Vision, 2010 Publication	<1 %
29	Sheng Lian, Zhiming Luo, Cheng Feng, Shaozi Li, Shuo Li. "APRIL: Anatomical prior-guided reinforcement learning for accurate carotid lumen diameter and intima-media thickness measurement", Medical Image Analysis, 2021 Publication	<1 %
30	ddd.uab.cat Internet Source	<1 %
31	hal.archives-ouvertes.fr Internet Source	<1 %
32	scholarcommons.usf.edu Internet Source	<1 %
33	www.amazon.com Internet Source	<1 %
34	www.ijset.com Internet Source	<1 %
35	Gamantyo Hendrantoro. "Cross-layer optimization performance evaluation of OFDM broadband network on millimeter wave channels", 2008 5th IFIP International Conference on Wireless and Optical	<1 %

Communications Networks (WOCN 08), 05/2008

Publication

Exclude quotes	On	Exclude matches	Off
Exclude bibliography	On		

Carotid Artery Segmentation on Ultrasound Image using Deep Learning based on Non-Local Means-based Speckle Filtering

GRADEMARK REPORT

FINAL GRADE

/100

GENERAL COMMENTS

Instructor

PAGE 1

PAGE 2

PAGE 3

PAGE 4

PAGE 5

PAGE 6